# Confocal unrolled areal measurements of cylindrical surfaces

A. Matilla[*a], C. Bermudez[a], J. Mariné[a], D. Martínez[a] , C. Cadevall[b], R. Artigas[b]
[a]Sensofar Tech SL
[b]Center for Sensors, Instruments, and Systems (CD6), Technical University of Catalonia (UPC)

## ABSTRACT

Confocal microscopes are widely used for areal measurements thanks to its good height resolution and the capability to measure high local slopes. For the measurement of large areas while keeping few nm of system noise, it is needed to use high numerical aperture objectives, move the sample in the XY plane and stitch several fields together to cover the required surface. On cylindrical surfaces a rotational stage is used to measure fields along the round surface and stitch them in order to obtain a complete 3D measurement. The required amount of fields depends on the microscope's magnification, as well as on the cylinder diameter. However, for small diameters, if the local shape reaches slopes not suitable for the objective under use, the active field of the camera has to be reduced, leading to an increase of the required number of fields to be measured and stitched. In this paper we show a new approach for areal measurements of cylindrical surfaces that uses a rotational stage in combination with a slit projection confocal arrangement and a high-speed camera. An unrolled confocal image of the cylinder surface is built by rotating the sample and calculating the confocal intensity in the centre of the slit using a gradient algorithm. A set of 360º confocal images can be obtained at different heights of the sample relative to the sensor and used to calculate an unrolled areal measure of the cylinder. This method has several advantages over the conventional one such as no stitching required, or reduced measurement time. In addition, the result shows less residual flatness error since the surface lies flat in the measurement direction in comparison to field measures where the highest slope regions will show field distortion and non-constant sampling. We have also studied the influence on the areal measurements of wobble and run-out introduced by the clamping mechanism and the rotational axis.

**Keywords:** confocal, unrolled 3D, microscopy, three dimensional measurements, optical inspection

## 1. INTRODUCTION

Confocal microscopes are widely used for areal measurements thanks to its good height resolution and the capability to measure high local slopes. For the measurement of large areas while keeping few nm of system noise, it is needed to use high numerical aperture objectives, move the sample in the XY plane and stitch several fields together to cover the required surface. Other technologies such as Coherence Scanning Interferometry (CSI) and Focus Variation (FV) [1] are also widely used for the measurement of technical surfaces. Each technology has its own advantages and disadvantages. For instance, Interferometry provides the highest vertical resolution independently of the numerical aperture of the objective, but it has the drawback of being highly sensitive to vibrations and requires a dense Z scan to extract the areal information. Focus Variation has the benefit of being very robust for the measurement of rough surfaces, but it requires high numerical aperture to achieve high vertical resolution. For low magnification objectives, Focus Variation is more suitable to measure the form and waviness components of a surface more than its texture, due to its limited lateral resolution [2].

When measuring cylindrical surfaces, an optical profiler cannot get the full topography along a full revolution. The sample has to be fixed on a rotational stage, and several topographies have to be acquired at different angles. The amount of individual topographies depends on the sample diameter and the field of view. Ideally, on a confocal microscope the use of a high numerical aperture will provide the highest resolution, but at the cost of very small field of view and larger amount of individual topographies compared to a low magnification, low numerical aperture objective.

*matilla@sensofar.com; phone +34 93 700 14 92; www.sensofar.com

On cylindrical parts the interest is not in the 3D shape of the cylinder itself, but in a given amount of spatial frequencies of the surface. Some of the characteristics of interest are the roughness, the shape deviation (form error) and the lead and twist analysis for example as defined in the Mercedes-Benz standard MBN 31 007-7 for the automotive industry. Figure 1 shows some of the above examples. This imposes the need to remove from the measurement the nominal cylinder that appears when stitching all the individual data. As far as we know, there are two approaches for stitching all the fields onto a single topography: stitching on the 3D space and removing the cylindrical shape, or removing the cylindrical shape of each individual topography and stitch all the data at the end.

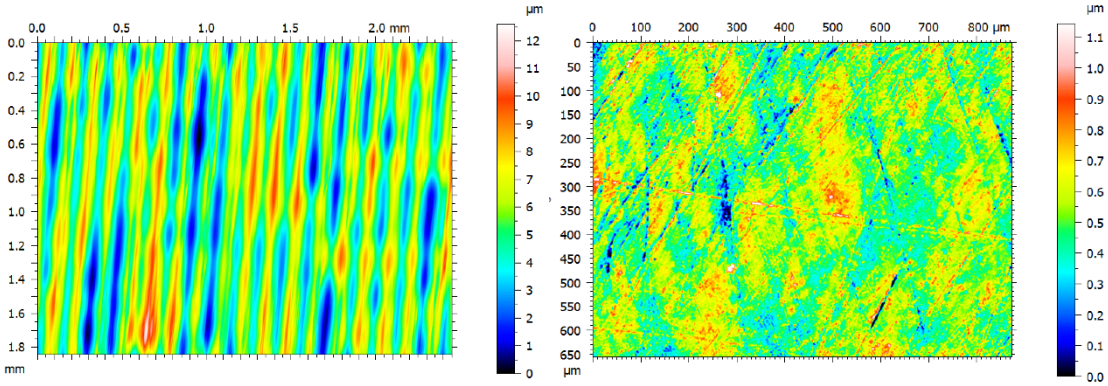


Figure 1. Typical helix pattern on a turned part for the automotive industry (left) where the helix period and angle are measured. (right) Roughness components on a bearing needle.

1. Stitching the individual data in the 3D space.

   This is the most common approach, since it provides a circular-like profile similar to a contact stylus profiler. The benefit of this approach is that the results can be shown on a polar plot, very useful if the characteristics of the surface intended to be analysed are mainly the waviness components. In an areal result, this approach cannot display the full data on a computer monitor, and the surface analysis cannot be performed on the 3D surface, but on individual cut profiles. Additionally, the stitching process requires good knowledge of the rotational angle where the data was taken. Any error in such value will end with a non-closed profile of the 3D object, forcing the stitching algorithm to increase the overlapping area or the nominal diameter, introducing spatial frequency errors that are not real from the surface. At the end of the stitching process, the 3D data can be be flattened on a 2.5D result using the best fit or nominal fit diameter, allowing further analysis.

2. Removing the cylindrical shape to all individual fields, and stitch them afterwards.

   The second approach on an areal measurement system is to remove the shape of the individual cylindrical fields prior to stitching. In contrast to the previous method, the final result naturally removes the main cylinder, and thus it is 2.5D in nature. Visualization and analysis of the results is straightforward, and the existing ISO 25178 filtering and analysis normative can be applied. There are two possibilities to remove the cylindrical shape for each individual field:

   2.1: Fitting a best fit cylinder: this has the advantage of literally flattening the result, at the cost of removing low frequencies that could be present on the surface. This method is well suited for roughness measurements.

   2.2: Fitting the nominal radius cylinder: this method removes the cylinder shape, but preserves the low frequency components. This is a good method for waviness measurements, but it has the drawback that the nominal value has to be very well known. Any deviation from the real value leaves a periodic residual shape that will be confusing waviness values [3].

   Figure 2 shows the result after measuring a glass rod of 10.0 mm nominal radius with a 10X 0.3NA objective. Figure 2 (a) shows the residual flatness error when removing the best-fit radius (in this case 5.2 mm), while (b) depicts the residuals after removing a cylinder of the nominal diameter.

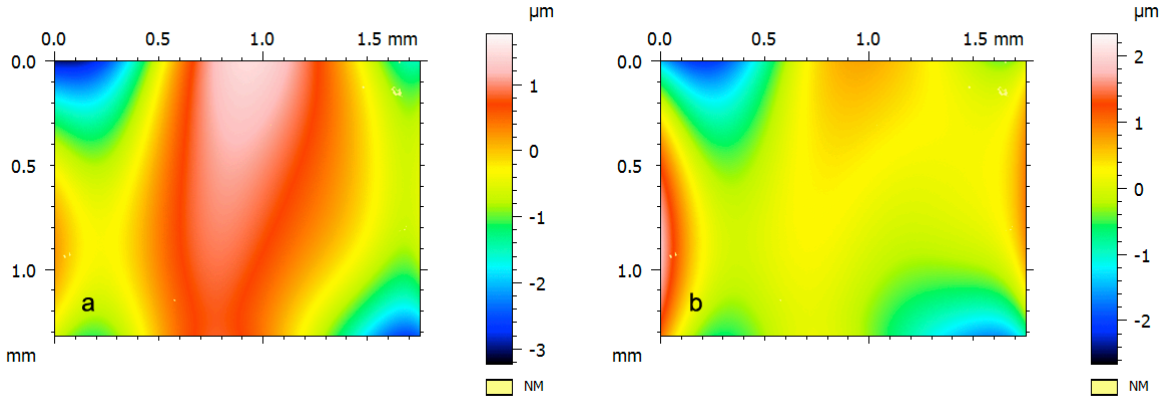


Figure 2. (a) Residual flatness error topography when removing a cylinder shape from a real measurement taken with a 10X 0.3NA objective. Nominal radius of 5.0 mm. (b) Best-fit radius of 5.2 mm.

Any of the above methods will suffer from an inherent limitation of the confocal technique related to the calibration process. Any confocal microscope is calibrated with a reference calibration mirror that is placed perpendicular to the optical axis [4]. A single topography is acquired showing a low frequency shape (similar to a sphere) related to the field curvature of the optical system. Such measurement is called flatness error, and is taken as a reference and automatically subtracted to any following measurement. Nevertheless, when the object imaged through the microscope is tilted, the effective numerical aperture changes along the pupil of the confocal microscope objective, and the field curvature changes. This makes the calibrated flatness error to be no longer valid, leaving an additional error, called residual flatness error [3]. Figure 3 shows this error for a 10X objective when measuring a tilted flat mirror with slopes of 1 (black), 5 (blue), and 10 (red) degrees respectively. As it can be seen, residual flatness error can leave up to several microns.

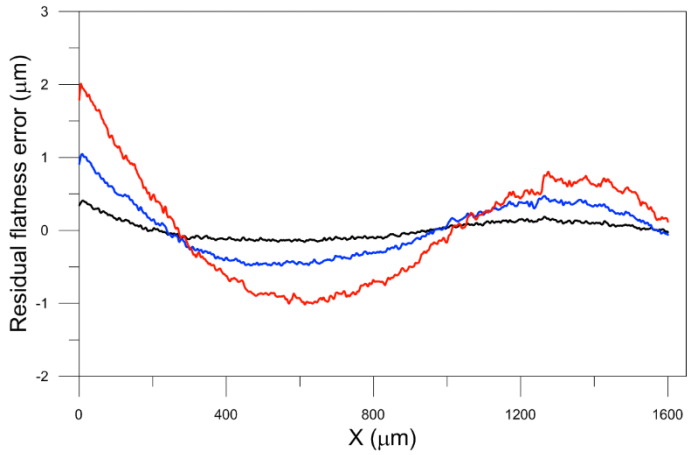


Figure 3. Residual flatness error with a 10X confocal objective when measuring a tilted flat mirror at 1 (black), 5 (blue), and 10 (red) degrees.

On a cylindrical sample, the residual flatness error will leave a low frequency component. The amplitude of the error is proportional to the local slope, and thus to the radius of the cylinder and the field of view of the microscope. For example, for a 10X objective with a FOV of 1.7 mm and a 10 mm diameter cylinder, the maximum slope will reach close to 10º. According to Fig. 3 shown before, the nominal deviation will show up to 3 µm, making the best fit sphere to have a higher repetitive error than the best fit. Figure 4 shows the residual flatness error on a cylindrical sample with 10.0 mm nominal diameter.

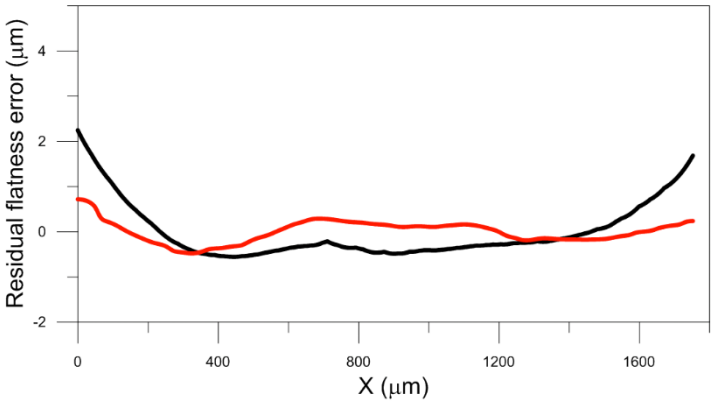


Figure 4. Residual flatness error on a cylindrical sample. Red: with best fit radius shape removal. Black: with nominal radius shape removal.

Stitching process will in any case leave a residual flatness error in a repetitive pattern that will be confused as a low frequency component of the surface, or as a repetitive waviness. This error can be calibrated and subtracted to every individual measurement, but calibration process will need to be known from low form error of cylindrical samples at several diameters, making the method not easy to implement. Figure 5 shows the residual flatness error on a cylindrical glass sample taken with a 10X objective and 10 field stitching after rotating the sample 20 degrees between fields.

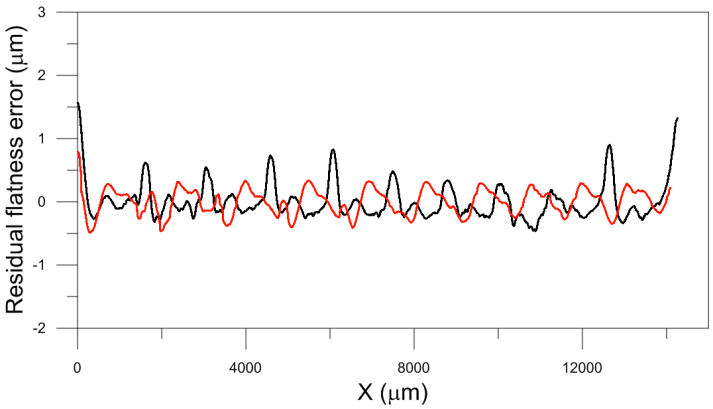


Figure 5. Residual flatness error on a cylindrical sample after stitching 10 individual fields. Red: with best fit radius shape removal. Black: with nominal radius shape removal.

In this paper we propose a new measurement method of cylindrical surfaces that will overcome the aforementioned effect. The basic idea behind it is to rely on the fact that cylindrical samples do not show high slopes in the direction of its revolution axis, making the residual flatness error to be minimal in that direction. The new method acquires an unrolled confocal image by grabbing on a single line parallel to the cylinder axis while rotating the sample at constant speed.

## 2. METHOD

On cylindrical surfaces a rotational stage is used to measure fields along the round surface and stitch them in order to obtain a complete 3D measurement. The required amount of fields depends on the microscope's magnification, as well as on the cylinder diameter. In addition, for small diameters, if the local shape reaches slopes not suitable for the objective under use, the active field of the camera has to be reduced, leading to an increase of the required number of fields to be measured and stitched. This is even more evident when measuring the cylinder shape with low magnification optics, where the maximum permissible local slope is relatively low, and thus the suitable used field of the camera is even smaller.

In this paper we show a new approach for areal measurements of cylindrical surfaces using a rotational stage in combination with a slit projection confocal arrangement and a high-speed CMOS camera. The slit is located on the field diaphragm position of the microscope and illuminated with an LED. Its image is projected onto the surface with a microscope objective. The reflected light goes back through the objective and is imaged onto a CMOS camera that can work as area-scan, or line-scan sensor at higher acquisition speed. An unrolled confocal image of the cylinder surface is built by rotating the sample and calculating the confocal intensity in the centre of the slit. We have tried two confocal approaches. The first one consists of recording the intensity of a single pixel or to the average sum of intensities in an evaluation window (defined perpendicular to the slit), depending on the magnification used. In our case, with a 10X 0.3NA we have used one single pixel. The recorded signal can be expressed as:

$$I(i,j) = \sum_{k=-N/2}^{k=N/2} p_{i,j+k} \tag{1}$$

being $i,j$ the coordinates of the pixel under evaluation, $p$ the pixel value, and $N$ the evaluation window size. The second method is the pixel gradient, corresponding to the square summation of the gradient values on the same perpendicular window.

$$G(i,j) = \sum_{k=-N/2}^{k=N/2-1} (p_{i,j+k+1} - p_{i,j+k})^2 \tag{2}$$

The whole optical sensor head is mounted on two linear stages corresponding to X and Z directions shown in Figure 6, allowing the sensor to move through the focal region of the microscope, and to position the cylinder along its main rotational axis. A rotation stage is mounted in parallel to the sample rotation axis, allowing the sample to be positioned in every angular position with high precision and rotate it at a constant speed for the line-scan approach.

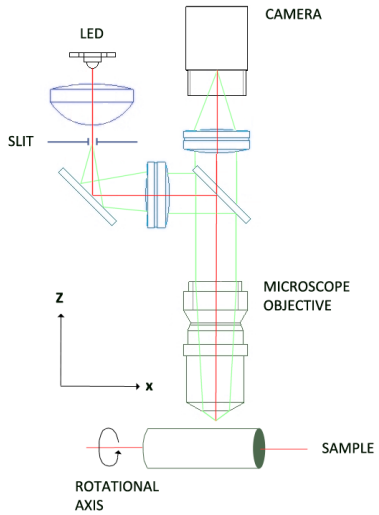


Figure 6. Schematic of the optical and mechanical setup to acquire unrolled confocal images.

A set of 360º confocal images can be obtained at different heights of the sample relative to the sensor and used to calculate an unrolled areal measurement of the cylinder. The benefits of this new approach in comparison to the field to field stitching are:

1. Measurement time is shorter
2. Nature of the unrolled data is 2.5D
3. No need to remove cylindrical shape as it is naturally removed by the acquisition method
4. Minimized flatness error
5. Preservation of the low frequency components achieving trustable waviness results
6. Uniform sampling due to constant perpendicular projection of the sample with the optical axis

The following figure shows two unrolled confocal images taken on a glass rod with a 10X 0.3NA objective. Both images were acquired on the same axial position. The first one corresponds to the direct, line-scan, intensity recording whereas the second is obtained with the gradient algorithm. Only a certain part of the image is on focus due to the run-out error of the rotation, which will be studied in the next section.

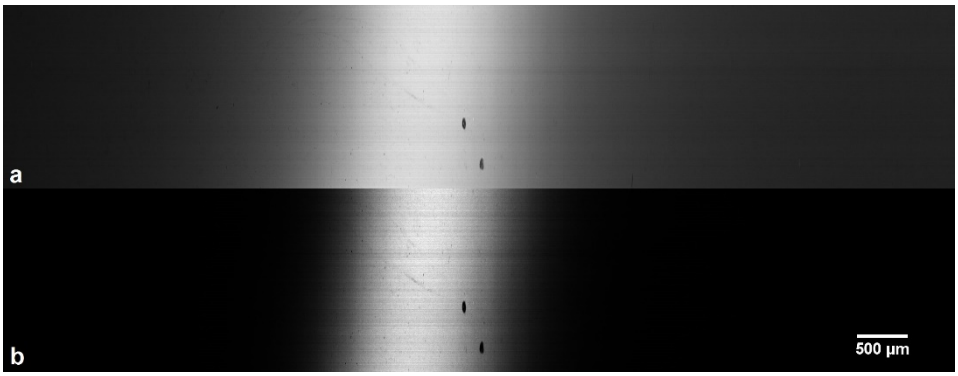


Figure 7. Confocal image of a line-scanned Ø10mm rod lens, obtained with two different approaches: (a) intensity recording, (b) gradient algorithm.

Gradient algorithm has higher optical sectioning than single pixel intensity. This behaviour can be seen on the intensity profile obtained from a single pixel along a Z scan, called the axial response. Figure 8 shows the comparison of the axial responses obtained from the intensity image and the gradient calculation performed on a single pixels and extracted through the series of confocal images taken along the depth of focus of the microscope.

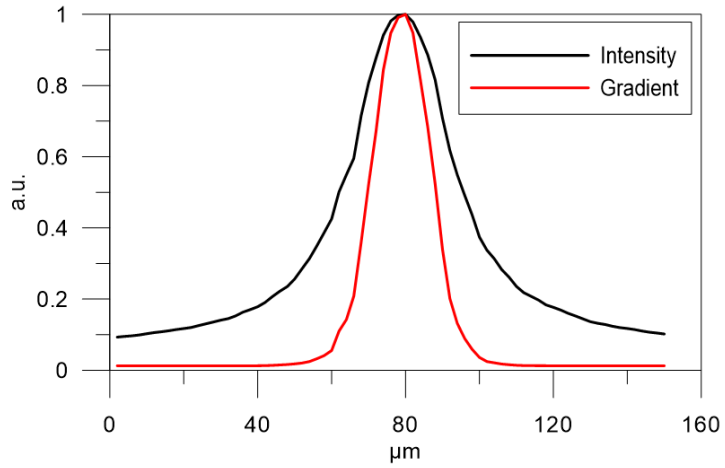


Figure 8. Axial responses of the two confocal imaging methods proposed for a 10X 0.3NA objective: image intensity and gradient.

## 3. ERROR INFLUENCES

We have studied the influence of the rotational axis on the areal measurements. In particular, the clamping mechanism will introduce to the final measurements circularity, cylindricity and concentricity errors that should be characterized and removed. The two major error sources that we have identified are the wobble and the total run-out introduced by the rotational axis and the clamping mechanism. This two errors manifest on the measured topography as low frequency components that correspond to the periodicity of a full turn of the surface. By identifying such form errors from the series of the confocal images, it is possible to predict their amplitude and isolate the components on the topography by subtracting them from the raw data. This method provides areal surface topography closer to the real one than any other existing method today.

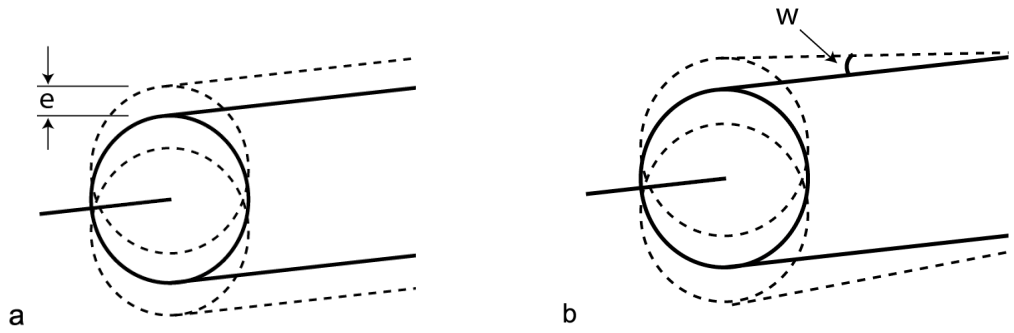


Figure 9. The two main error sources coming from the rotational axis and the clamping mechanism are: (a) run-out and (b) wobble.

In the case that only run-out is present, the sample will shift from focus position as it turns along its axis. This translates to the unrolled confocal image as a bright region where the sample is located in focus, and progressively goes out of focus as it turns, being the largest distance to focus on the opposite direction. Figure 10 depicts the effect of run-out.

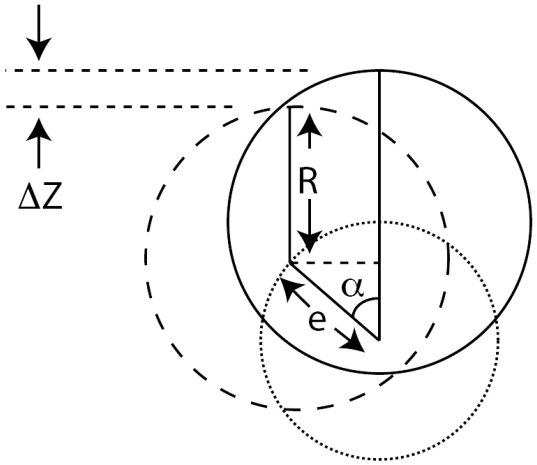


Figure 10. Focus error (Δz) due to run-out (e) of the rotation stage.

where $\Delta z$ is the focus error, $R$ the radius of the sample, $e$ the run-out error, and $\alpha$ the angle were the focus distance is evaluated. The focus error is described by:

$$\Delta z = e * (1 - \cos(\alpha)) \tag{3}$$

The previous equation describes that in the presence of run-out, the final topography will have a sinusoid-like component with an amplitude $e$, which will be mainly due to this error source. It is a straightforward process to fit a sinusoidal function, and subtract it from the topography. Figure 11 shows a simulation of a series of confocal images taken on a glass rod with a 10X 0.3NA objective where the run-out effect is clearly visible. The final topography, shown in Figure 12, which should be flat (cylindrical shape is naturally removed by the acquisition method) is exhibiting such low frequency component with amplitude of 10 μm.

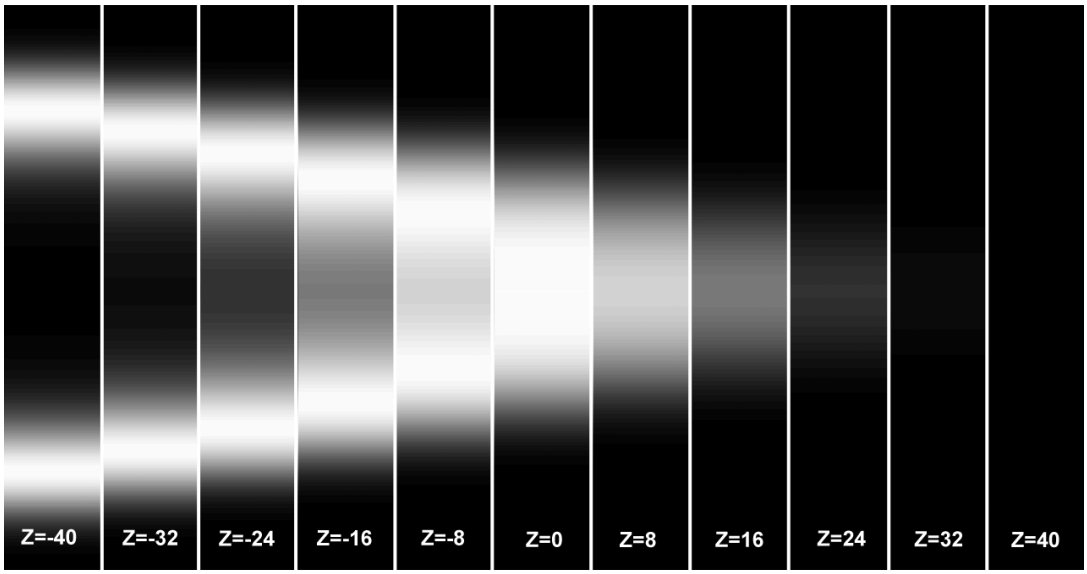


Figure 11. Simulation of a series of 11 confocal images of a glass rod taken with a 10X 0,3NA objective, and a run-out error *e* of 10 µm. The vertical scan is +/- 40 µm.

The topography calculated from the series of images of Fig. 11 can be seen in the following figure:

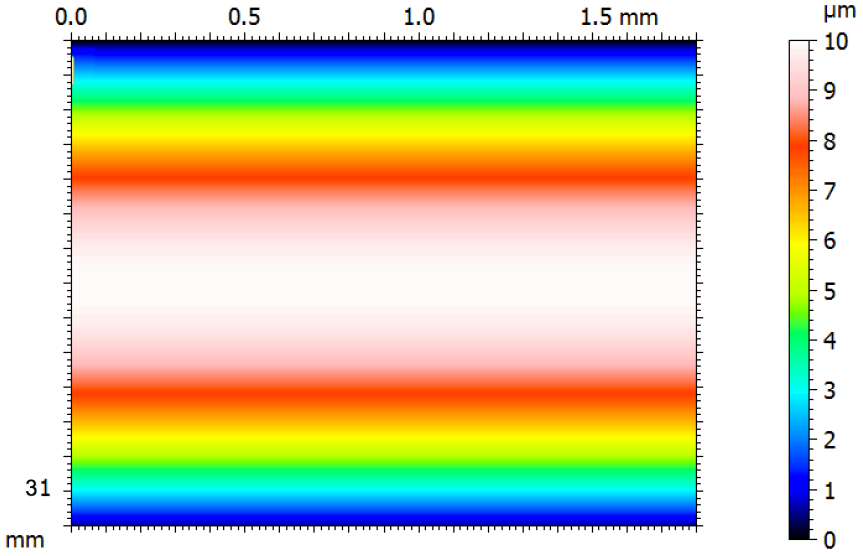


Figure 12. Calculated topography with a run-out *e* of 10 µm. The residual error is a low frequency component. XY axes have a different scaling in order to preserve a low aspect ratio.

In the presence of wobble, it is straightforward to understand that it will equal to a run-out that increases in amplitude as its distance to the clamping mechanism increases. Equation 3 describes this case:

$$\Delta z = (e + \tan(w) * X) * (1 - \cos(\alpha)) \tag{4}$$

being *e* the system run-out, *w* the wobble angle, and X the direction along the cylinder axis. In this case the series of confocal images will have the same sinusoid appearance, but the amplitude will increase along the X axis. Figure 13 shows a simulation of a series of images obtained with the same settings as Fig. 11 but with a wobble of 1º.

The final topography is shown in Figure 14. Like in Fig 12 it should be flat (cylindrical shape is naturally removed by the acquisition method) but is exhibiting the wobble error as a low frequency component with amplitude of 10 µm.

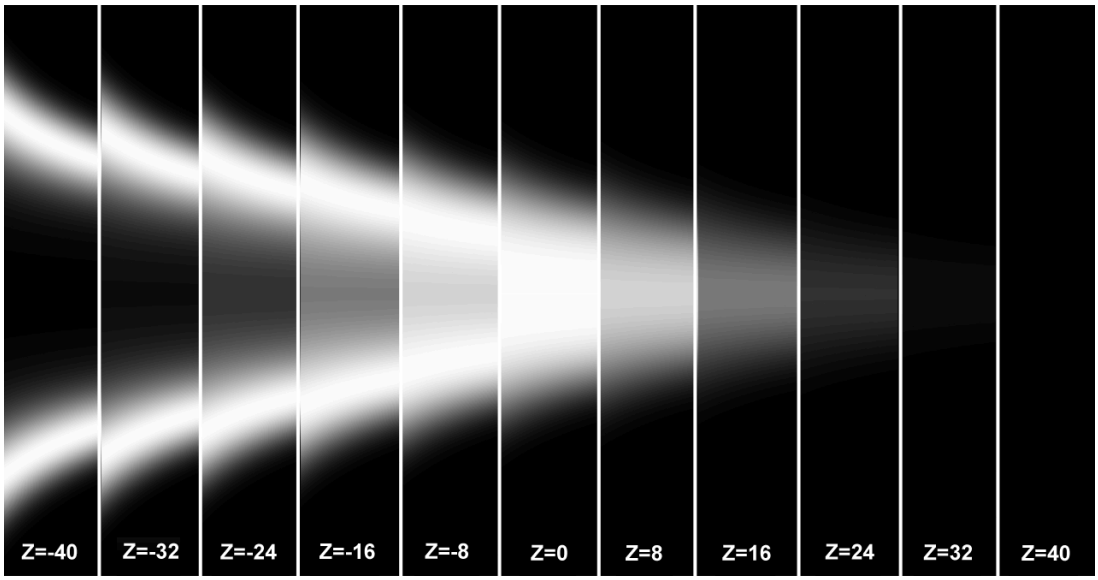


Figure 13. Simulation of a series of 11 confocal images of a glass rod taken with a 10X 0,3NA objective, with a run-out error *e* of 10 µm and a wobble *w* of 1º. The vertical scan is +/- 40 µm.

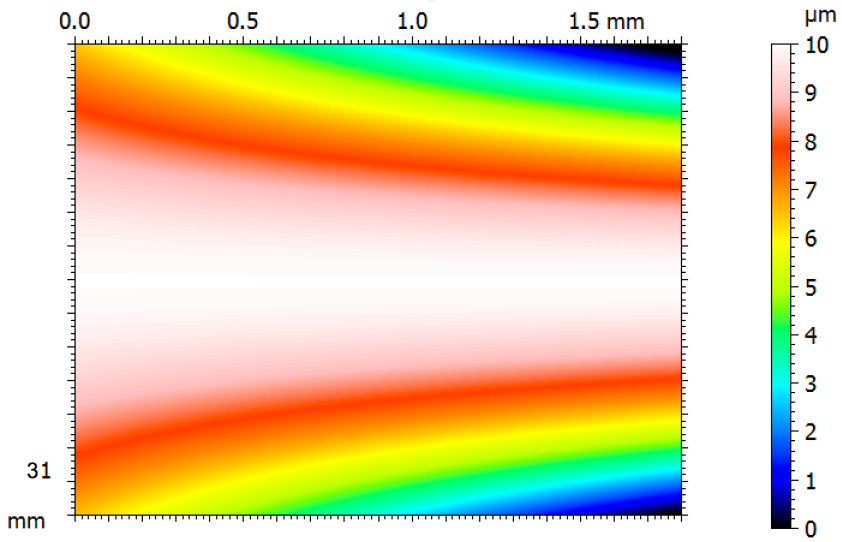


Figure 14. The calculated topography with a run-out of 10 µm and a wobble of 1º. The residual error is a low frequency component. XY axes have a different scaling in order to preserve a low aspect ratio.

In order to verify the previous simulation, a real measurement was taken on a glass rod of 10 mm diameter and a 10X 0.3NA objective. Figure 15 (a) shows the measurement of such sample with a clear run-out, and slightly visible wobble. Figure 15 (b) shows the residuals after fitting a sinusoid-like topography coming from run-out and wobble errors (Eq. 4). Some residual frequencies are still visible, being most of them from the surface. As it is clearly shown, the residual error has been decreased from 20 µm PV to less than 0.8 µm, which clearly demonstrates the benefit of removing the residual errors from a well-known shape form.

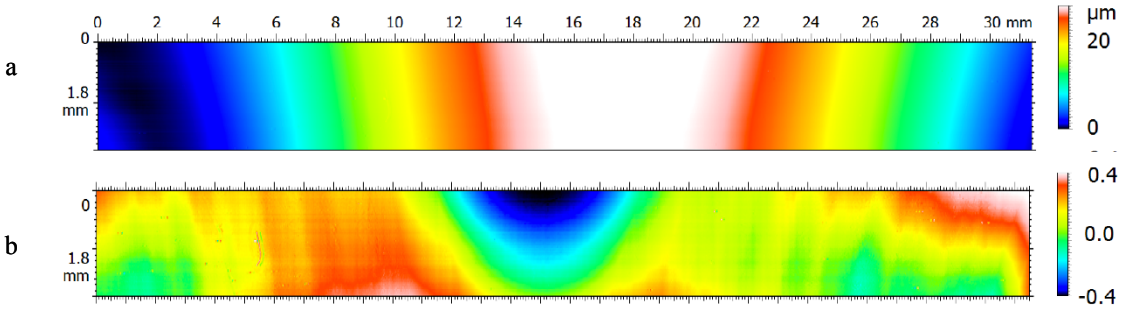


Figure 15. (a) Unrolled topography of a glass rod of 5 mm diameter taken with a 10X 0.3NA objective. (Bottom) residual topography after removing a best fit of run-out and wobble errors (equation 4). The PV has been reduced from 20 to 0.8 micron.

## 4. RESULTS

To proof the concept of unrolled areal measurements, we have used a Basler acA2000-50gc camera mounted on a 0.5X field lens, and a slit of 15 micron width projected onto the surface. A turned brass part of 4.0 mm in diameter is hold on a 1000 steps/revolution stepper motor, model Orientalmotor PKP544MN18A and driven with a 1:250 microstepping controller. The camera is triggered at 1000 frames per second and 7 rows of pixels centred on the slit have been acquired. We used a 10X 0.3NA microscope objective to acquire the unrolled confocal images, and optimum Z increment steps of 2.0 µm to get a series of images. Every unrolled confocal image started at the same sample angle. Stepper motor controller generates an acceleration profile and triggers the camera for the first time to start image acquisition as soon as the motor is rotating at the nominal speed. Although being hardware-controlled, still some repeatability mismatch during the acquisition start trigger made the confocal images to be vertically shifted a few pixels. Therefore, after the acquisition, we have registered all the confocal images sequence with a translation-only registration algorithm, making every pixel in the Z stack to belong to the same point in the image.

Figure 16 shows the unrolled topography of a brass turned part. The helix shape is clearly visible, as well as the low frequency components coming from the run-out of the rotational stage. Figure 16 (a) shows the original topography while (b) is the best fitting corresponding to run-out and wobble errors (equation 4), exhibiting the sinusoidal error shape.

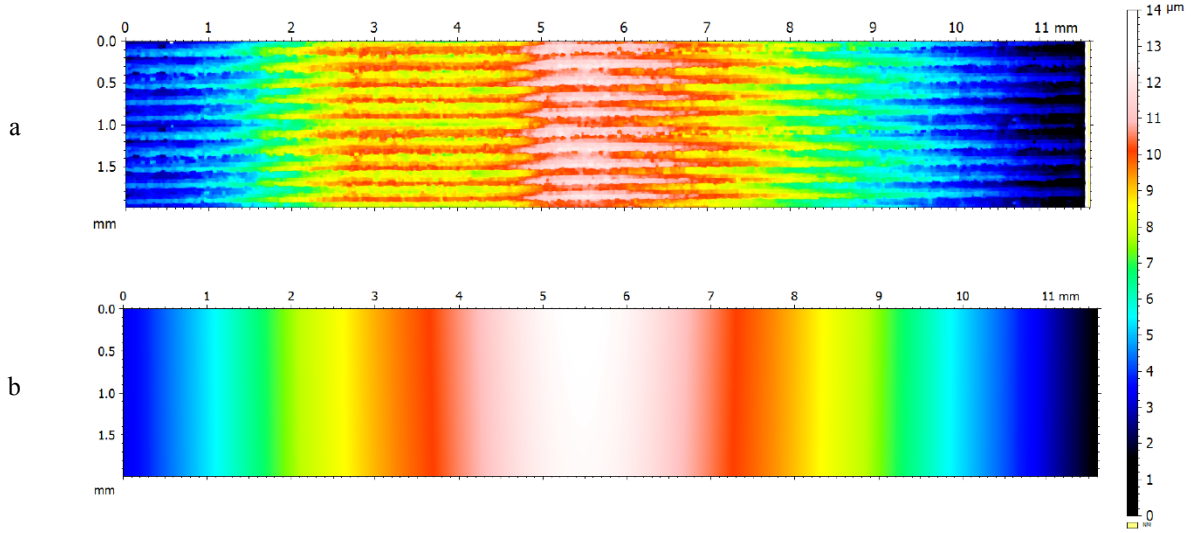


Figure 16. Unrolled topography of a turned brass cylinder of 4 mm diameter. (a) Original topography, (b) the best-fit from run-out and wobble errors (Eq. 4).

The difference of the two previous figures is shown in Figure 17:

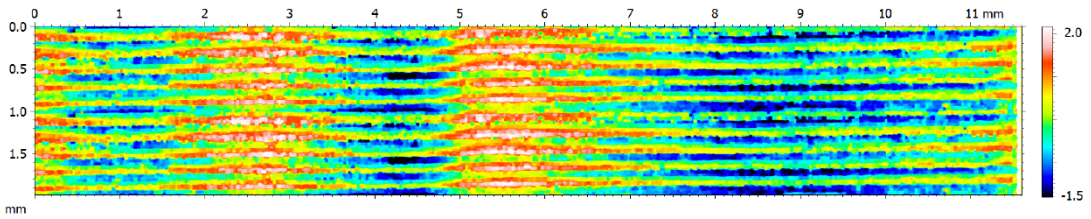


Figure 17. Unrolled topography of a turned brass cylinder of 4 mm diameter after removing the best-fit error from Eq. 4.

Finally, a cut profile of the previous figure in the Y direction is shown in Figure 18.

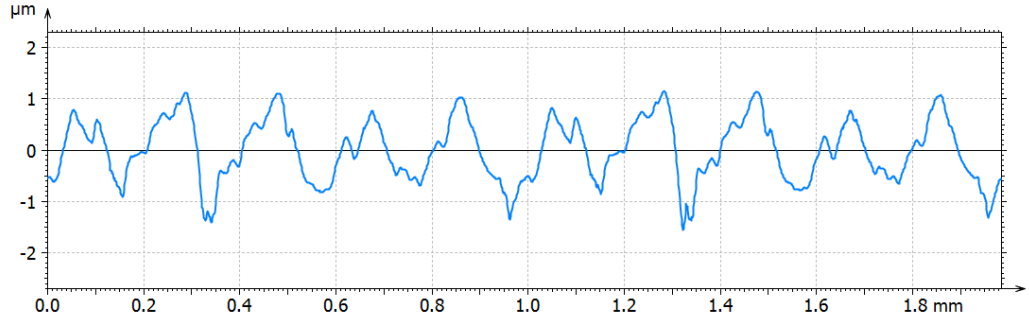


Figure 18. Profile cut from figure 17 in the X direction.

## 5. CONCLUSIONS

In this paper we have discussed the residual flatness error appearing in imaging confocal microscopes when measuring cylindrical parts. We have reviewed the stitching approaches to measure turned parts and how the residual error leaves low frequency components that are not from the surface under inspection. To overcome this problems we have shown a new optical measurement approach based on confocal microscopy for the measurement of cylindrical surfaces. This new optical method uses a slit projection and a rotational axis to acquire a series of unrolled confocal images and recover the 2.5D surface topography. The method shows several advantages in front of conventional measuring methods such as no required stitching, reduced flatness error, and increased speed to minimize overall measurement time. We have also analyzed the source of the errors of this new acquisition approach and proposed a mathematical correction method.

## REFERENCES

[1] Leach R. “Optical Measurement of Surface Topography,” Springer Verlag ISBN 978-3-642-12012-1

[2] Claudiu L. Giusca, James D. Claverley, Wenjuan Sun, Richard K. Leach, Franz Helmli, Mathieu P.J. Chavigner. “Practical estimation of measurement noise flatness deviation on focus variation microscopes,” CIRP annals – Manufacturing Technology 63 (2014)

[3] Sensofar Tech App. Note. “Flatness error on Imaging Confocal Microscopes,” (2009), http://www.sensofar.com/references/FlatnessError.pdf (11 April 2017).

[4] Claudiu L. Giusca, Richard K. Leach. “Calibration of the scales of areal surface topography-measuring instruments: part 1. Measurement noise and residual flatness,” Measurement Science and Technology (2012).